

# We are IntechOpen, the world's leading publisher of Open Access books Built by scientists, for scientists

6,900

Open access books available

186,000

International authors and editors

200M

Downloads

Our authors are among the

154

Countries delivered to

TOP 1%

most cited scientists

12.2%

Contributors from top 500 universities



WEB OF SCIENCE™

Selection of our books indexed in the Book Citation Index  
in Web of Science™ Core Collection (BKCI)

Interested in publishing with us?  
Contact [book.department@intechopen.com](mailto:book.department@intechopen.com)

Numbers displayed above are based on latest data collected.  
For more information visit [www.intechopen.com](http://www.intechopen.com)



# Suppression of Corrosion Growth of Stainless Steel by Ultrasound

Rongguang Wang

*Department of Mechanical systems Engineering, Faculty of Engineering,  
Hiroshima Institute of Technology,  
Japan*

## 1. Introduction

Metals are smelted from natural minerals and they tend to return back to their original or stable states including oxides and hydroxides. One of the later processes is corrosion, which occurs from metal surfaces with surrounded air or electrolytes. With the propagation of corrosion, the metal becomes thin as well known as the uniform corrosion of carbon steels, holes appear from the surface such as pitting corrosion of stainless steels, or cracks initiate and propagate from or in the metal like stress corrosion cracking, hydrogen embrittlement or corrosion fatigue. In many cases, cracks initiate from pitting corrosion. Either of the above phenomena leads certainly to the strength loss of metals and accordingly largely shorten the structures' life. Before carrying out a maintenance of metallic structures, the ultrasound is frequently used to investigate the degradation level of the structures by comparing the emitted and the reflected waves. Many researches and applications have been carried out on this topic.

On the other hand, in comparison with the prediction of the residual life and the maintenance of structures, it is much more important to stop or retard the initiation of corrosion; at least the propagation of corrosion should be effectively suppressed to thoroughly prolong the structures' life. This is generally solved by increasing the thickness of the applied steels, using high grade steels containing expensive or rare elements of chromium, nickel and molybdenum, or changing the surroundings of air or electrolytes. In this topic, a new method of using ultrasound to suppress the corrosion of stainless steel was introduced.

## 2. Corrosion process of stainless steel with formation of corrosion products

The high corrosion resistance of stainless steels originates from the formation of a passive film on the surface. In general, much oxide and hydroxide of chromium are contained in the passive film. However, the pitting corrosion or the crevice corrosion often occurs when the passive film is locally broken down by the chloride ions in solutions. The researches to retard the pitting initiation and growth have elapsed for near one century since the birth of stainless steel. In general, during the corrosion reaction, the metal surface will be separated into cathode zones and anode zones. On the cathode zones, the reduction reactions occur generally with the transformation of hydrogen ions to hydrogen gas or the transformation of oxygen gas to hydroxide ions, where the loss of metal does not occur. On the anode

zones, the oxidization reactions occur with the transformation of metals to metallic ions into the solution, which means the loss of metal. The total reaction on the anode zones is equal to that on the cathode ones. When either of the anode or the cathode reaction was suppressed, the corrosion propagation should be slowed down. In the pitting corrosion, the area of cathode zones is much larger than the anode ones, which results in that even small cathode reaction rate can induce deep pit formation.

The main characteristic of pitting corrosion is that the thickness of the steel almost does not verify, while in some places holes form from the surface and sometimes penetrate the whole steel. The formation of the holes (hereinafter called as pits) includes the initiation stage and the growth stage. It is very important to suppress both the initiation and the growth of stainless steels to prolong the life of machines and structures. The stainless steel generally contains chromium and nickel with the balance of iron. The widely used typical austenite stainless steel is the type 18-8 steel (also being called as SUS304 steel or Type 304 steel), where 18mass% Cr and 8% Ni were contained with a little of carbon less than 0.08%. In the initiation of pitting corrosion of stainless steel, the Cl<sup>-</sup> ions generally concentrate to weak sites of the passive film, under which always impurities such as MnS, MnO, Al<sub>2</sub>O<sub>3</sub>, TiO<sub>2</sub> and others exist (Ryan et al., 2002; Shimizu, 2010a, 2010b; Yashiro & Shimizu, 2010). In comparison to other zones with good state of passive film, the potential of such weak sites is somewhat lower, which promotes to form micro cells where the weak sites act as the anodes and other wide zones become the cathodes. This induces the acceleration of anode reaction at such weak sites, where pits initiate. The pit growth is always accompanied by the corrosion product of oxides and hydroxides of metals covering the pit, which accelerates the pit growth by promoting the accumulation of hydrogen and chloride ions into the pits, i.e., excessive hydrogen ions are produced in the pit with the hydrolysis reaction and the chloride ions migrate from outside to neutralize the excessive positive charges (Hisamatsu, 1981).

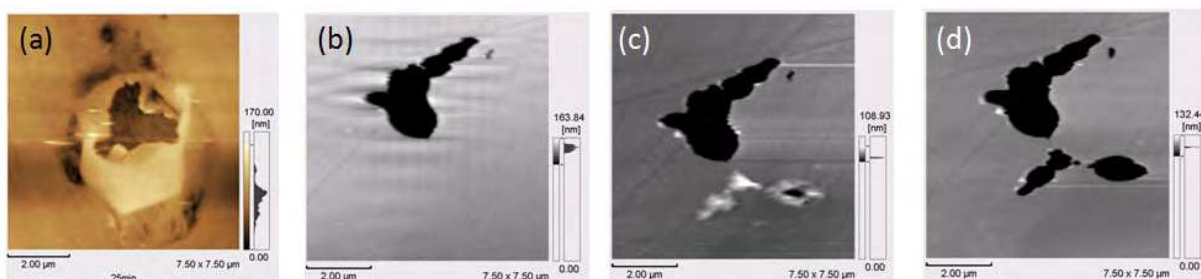


Fig. 1. Corrosion products on Type 304 stainless steel in 3.5% NaCl solution, in-situ observed by atomic force microscopy. Copyright 2005 Elsevier

The corrosion product on Type 304 steel in 3.5 mass% NaCl solution during the pitting corrosion was in-situ observed at room temperature by atomic force microscopy (AFM), as shown in Fig.1 (Zhang et al., 2005). A corrosion product crust covered perfectly a small pit at its initiation stage. Part of the corrosion product was then removed by the scanning probe of AFM (Fig.1 (a)). After the break of the corrosion product crust, the pit did not grow more. Fig.1 (b-d) shows several irregular pits formed near chromium carbides. With the increase in the corrosion time, a corrosion product and a small elliptical pit with corrosion product around it were observed (b, c). Almost all the corrosion products were removed by the probe of AFM and two small pits clearly appeared there (d). After then, their shapes did not change anymore. The retardation of pit growth is explained by the decrease in the

concentration of chloride and hydrogen ions in the pit due to the destruction of the crust and the stirring of the solution in the pit by the probe. As a result, re-passivation on the inner surface of the pit easily occurred and the corrosion almost stopped.

### **3. Promotion or suppression of corrosion of steels by ultrasound (Wang & Kido, 2009)**

If there is a simple method to remove the corrosion product covering pits, the growth of pits can be suppressed even for the cheap and low grade stainless steels. Here comes the idea of using ultrasound (US) to achieve this aim. The ultrasound in liquids always induces acoustic cavitation (Chouonpa Binran Henshu Iinkai(CBHI), 1999). In the acoustic cavitation, bubbles generate, grow and collapse due to the extremely increased internal tensile and compressive stress in the liquid. The cavitation power relates to the frequency and the amplitude of ultrasound as well as the type of liquid. It is widely used to clean solid surfaces, disperse powders and accelerate chemical reactions in liquids. The acceleration of chemical reactions is mainly caused by the high internal pressure and high temperature in the cavitation.

It is frequently reported that the erosion or corrosion rate on metal surfaces in specific liquids can be promoted by the acoustic cavitation. Alkire et al studied the passivity of iron in 2 N H<sub>2</sub>SO<sub>4</sub> solution and found that iron became active when a focused ultrasound was applied in the solution (Alkire & Perusich, 1983). Al-Hashem et al investigated the acoustic cavitation corrosion behaviour of cast Ni-Al-Cu alloy in seawater. Both the cathodic and anodic current of the alloy increased by an order of magnitude and the rate of mass loss increased near 186 times under the application of a 20 kHz ultrasound (Al-Hashem et al., 1995). Whillock et al measured the corrosion behaviour of 304L stainless steel in 2 N HNO<sub>3</sub> solution containing a small amount of Cl<sup>-</sup> at 323 K. The corrosion rate increased in the active state and the breakdown of passive film was promoted when a 55 kHz and 380 kW/m<sup>2</sup> ultrasound was applied with a vibrator-to-specimen distance of 1.1 mm (Whillock & Harvey, 1996). Kwok et al studied the cavitation erosion and corrosion characteristics on various engineering alloys including the grey cast iron, mild steels and stainless steels in 3.5% NaCl solution at 300 K when a 20 kHz ultrasound was applied. They found that corrosion mainly occurred on mild steel and grey cast iron but was negligible on stainless steel. The stainless steel only suffered pure mechanical erosion in the presence of cavitation (Kwok et al., 2000). Whillock et al also investigated the corrosion behaviour of 304L stainless steel in an ultrasonic field with different frequencies, acoustic powers and vibrator-to-specimen distances (Whillock & B.F. Harvey, 1997). At 20 kHz, the corrosion rate increased continuously with the increase in the power, while at the frequency of 40 to 60 kHz, the corrosion rate increased to the maximum and thereafter decreased with the increase in the power. The corrosion rate increased with the decrease in the vibrator-to-specimen distance, high corrosion rate in excess of 800 mm/year were obtained when the distance was 0.1 mm.

On the other hand, several papers reported that the corrosion on stainless steel can also be suppressed by the application of ultrasound in chloride containing solutions (Nakayama & Sasa, 1976; Whillock & Harvey, 1996; Wang & Nakasa, 2007; Wang & Kido, 2008; Wang, 2008). Nakayama and Sasa measured the polarization curves of a 304 type stainless steel in 0.1 N NaCl solution when applying a 200 kHz and 38-46 kW/m<sup>2</sup> ultrasound with a vibrator-to-specimen distance of 60 mm (Nakayama & Sasa, 1976). They found that the critical pitting potential became noble in the applied ultrasound field. Whillock et al found that ultrasound

can encourage the passivation of 304L stainless steel in 2 N HNO<sub>3</sub> containing small amounts of Cl<sup>-</sup> (Whillock & Harvey, 1996). Wang et al investigated the detail of the suppression effect of ultrasound on stainless steel in chloride solution (Wang & Nakasa, 2007; Wang & Kido, 2008; Wang, 2008; Wang & Kido, 2009; Wang, 2011).

The above conflicted influences of ultrasound on the corrosion behaviour of metals should be caused by (1) the type of metal, (2) the type of solution, (3) the acoustic power (frequency and amplitude) of ultrasound and (4) the ultrasound vibrator-metal distance. Especially, for stainless steels pitting corrosion and crevice corrosion usually occur when the passive film is locally broken down in chloride containing solutions. When the acoustic cavitation is strong enough, the passive film can be damaged and thus corrosion is activated. However, when the acoustic cavitation is not strong enough to damage the passive film the corrosion will not be accelerated. The suppression effect of acoustic cavitation on the pitting corrosion of stainless steel should be similar with that of the scanning of AFM probe in (a) the removal of the corrosion products (including the removal of the metallic cover under relatively larger power of ultrasound) and (b) the stirring of the solution in the pits. Of course, both of the removal and the stirring effects finally depend on a suitable power of the acoustic cavitation.

#### **4. Suppression of pitting corrosion on stainless steel by ultrasound (Wang, 2008)**

A trial was carried out to use ultrasound to remove the corrosion products covering pits, and the growth of pitting corrosion on Type 304 stainless steel was investigated in 3.5% NaCl solutions at 308 K. Pitting corrosion tests were carried out by using a corrosion cell attached with potentiostat apparatus (Hokuto Denko. Co., HAB-151) and an ultrasound cleaner (Yamato Co., Branson 2510J-MTH, 100 W, 42 kHz) as shown in Fig.2 (a). The counter electrode was platinum and the reference electrode was saturated calomel electrode (S.C.E.). The polarization was started from the cathode side ( $E_{S.C.E.} = -600$  mV) to the anode side at a constant potential increasing rate of 50 mV/min under the control of the potentiostat. With the linear increase in potential, the current changes from the cathode and passive zone to the pitting zone where the current density largely increases with a small increase in potential (Fig.2 (b)). When the anodic current density reached a value of  $i_h = 20$  A/m<sup>2</sup> in the pitting zone, the potential was immediately held constant for 600 s. In this way, the deviation of current density caused by different pitting potentials on different surfaces will be small. The ultrasound (nominate intensity: 3 kW/m<sup>2</sup>) was applied in 3 types of conditions, i.e., (i) without ultrasound (hereinafter called as condition A); (ii) applying ultrasound simultaneously with the holding of potential (condition B); (iii) applying ultrasound from the beginning to the end of the polarization (condition C). The potential corresponding to the above constant current density was kept for 600 s in all conditions.

For the polarization curves in conditions A, B and C, the current density changes from the cathode to the anode near the potential  $E = -150$  mV irrespective of the application of ultrasound. No significant difference was found in the corrosion potential and in the current density in the cathode zone and the anodic passive zone. This indicates that the ultrasound is not strong enough to break the passive film down, or the partially broken passive film can be easily self-repaired.

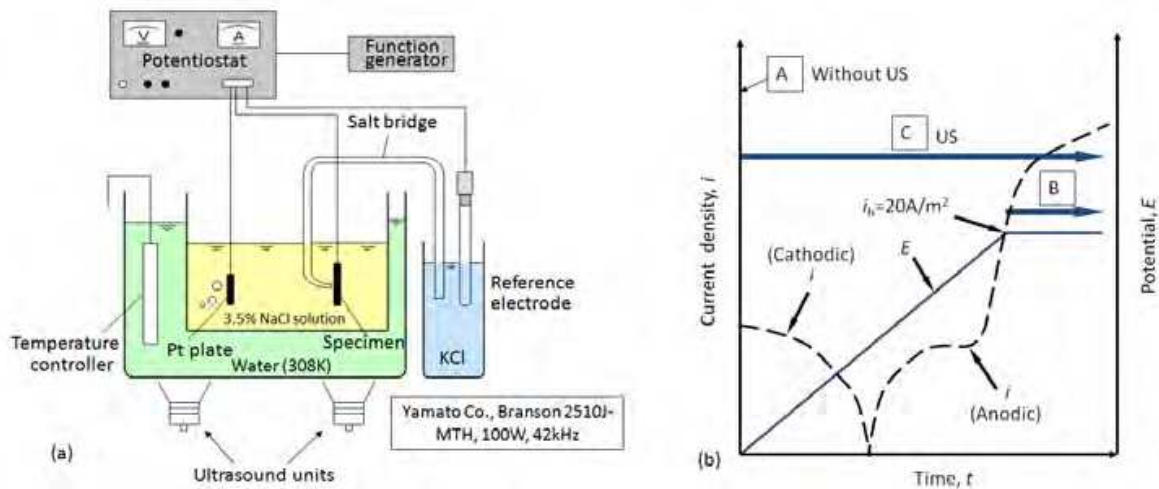


Fig. 2. (a) Polarization apparatus and (b) timing of ultrasound. Copyright 2008 Elsevier

The influence of ultrasound on the corrosion behaviour was observed mainly in the pitting zone. Fig.3 (a) shows parts of the polarization curves from  $i_h = 20 \text{ A/m}^2$ , where the vertical axis is shown in a normal decimal scale. It is clear that the current density in condition A is much higher than those in conditions B and C. This means that the pitting growth can be largely suppressed by applying ultrasound in solution. On the other hand, no large difference can be found in conditions B and C, which means that ultrasound is only effective after corrosion has occurred. Fig.3 (b) shows the typical surface morphologies of specimens after polarization and the electric charge calculated by the integration of the current density during the 600 s holding of potential after the current density reached  $i_h = 20 \text{ A/m}^2$ . The area of pits was measured from enlarged photos. The electric charge means the dissolution amount of metal ions into solution. Fewer pits were found on the surface with ultrasound, corresponding to the smaller electric charge.

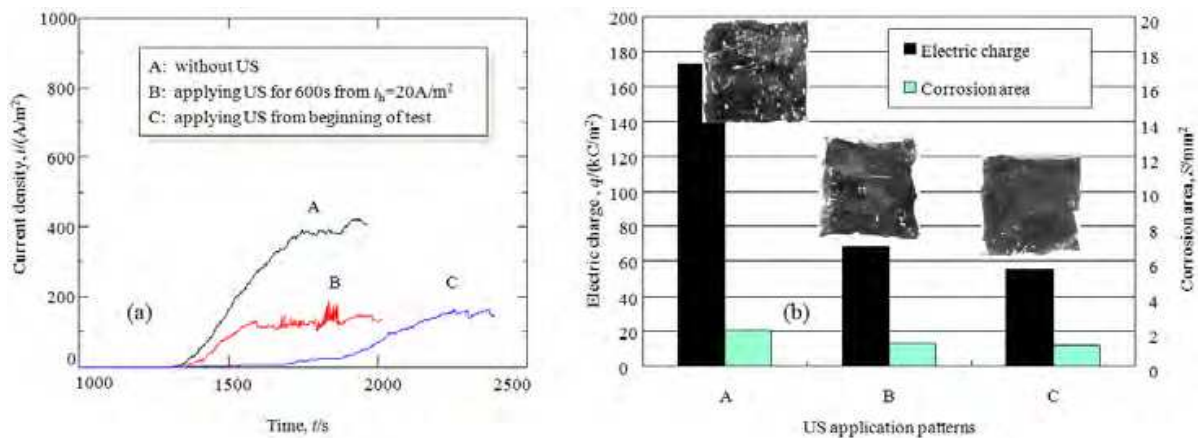


Fig. 3. (a) Change of anodic current density from  $i_h = 20 \text{ A/m}^2$ , and (b) electric charges for the 600 s holding from  $i_h = 20 \text{ A/m}^2$ . Copyright 2008 Elsevier

The mechanism is schematically shown in Fig.4. When the ultrasound is not applied, pits grow on the specimen surface (a) and corrosion product covers the pit (b) (Wranglen, 1985; Zhang et al., 2005). The growth of pit is accelerated due to the hydrogen ions produced by hydrolysis reaction and the chloride ions attracted from solution (c) (Wranglen, 1985). When the ultrasound is applied to the specimen surface, the corrosion product is removed by the

cavitation of ultrasound (b'). The concentration of corrosive hydrogen ions and chloride ions decreases due to the stirring effect of cavitation, and the growth rate of pits decreases (c').

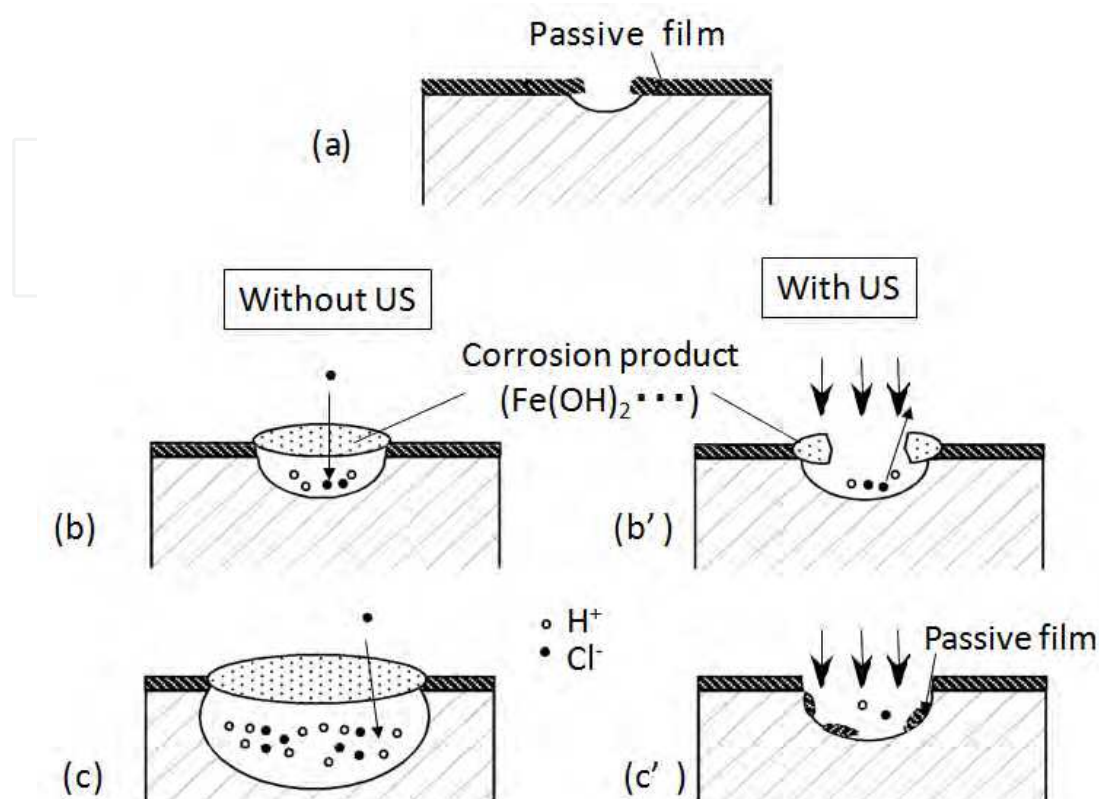


Fig. 4. Decrease in growth of corrosion pits by ultrasound. Copyright 2007 The Japan Institute of Metals

### 5. Suppression of crevice corrosion on stainless steel by ultrasound (Wang & Kido, 2008)

The mechanism of crevice corrosion is similar with pitting corrosion. In this section, the influence of ultrasound on the crevice corrosion will be introduced. Type 304 specimens were polished with the # 600 emery paper on both sides and then assembled by the following JIS G0592 standard (Japanese Industrial Standards Committee (JISC), 2002) to produce a crevice between the twice polished surfaces. The crevice was wetted by the 3.5% NaCl solution and tightened hardly by titanium nuts and washers to form the artificial crevices. Of course, there were also two small crevices between steel / washer. The corrosion test was carried out in a corrosion cell connected to a potentiostat (Hokuto Denko Co.; HAB-151) and an ultrasound cleaner (Yamato Co., Branson 2510J-MTH; 100 W, 42 kHz), as is shown in Fig.5. Hereinafter,  $i_h$  and  $i_u$  mean the current density when the potential was held constantly and the current density when the ultrasound was triggered, respectively.  $\Delta t_h$  and  $\Delta t_u$  mean the period for holding the potential constantly and the period for applying ultrasound, respectively.

Fig. 6 shows the change of the current density when the current density reached  $i_h = 10$  A/m<sup>2</sup> and the potential at that moment was held for  $\Delta t_h = 0.9\sim 1.2$  ks. The arrow ( $\Rightarrow$ ) shows the period for the application of ultrasound. The solid line (a) shows the result without

ultrasound, the broken line (b) shows the result when ultrasound was stopped after  $\Delta t_u = 0.6$  ks but the potential was continuously kept constantly for further  $\Delta t_h = 0.3$  ks, the dotted line (c) shows the result with ultrasound during the overall potential holding period ( $\Delta t_h = 1.2$  ks). In the case of (a), the current density largely increased near  $t = 0.9\sim 1.1$  ks ( $E = 470\sim 530$  mV) after the passive zone. After the polarization, no pitting corrosion can be observed and only crevice corrosion appeared (see Fig.7), i.e., the increase in the current density means the happening of crevice corrosion. The potential was about  $E_h = 488\sim 570$  mV at the moment of the crevice corrosion current density  $i_h = 10$  A/m<sup>2</sup>. During this period, the current density continued to rise slowly and finally kept almost stable at a value of about 200 A/m<sup>2</sup>. In the case of (b), the current density almost kept stable at the level of about 40 A/m<sup>2</sup>. This low and stable current density should be attributed to the dilution of the enriched Cl<sup>-</sup> and H<sup>+</sup> in the crevice caused by the stirring effect of ultrasound. When the ultrasound was stopped after 0.6 ks, the current density increased. It will be due to the re-enrichment of Cl<sup>-</sup> and H<sup>+</sup> because the disappearance of ultrasound. However, in the case of (c), the current density kept stable at a low level.

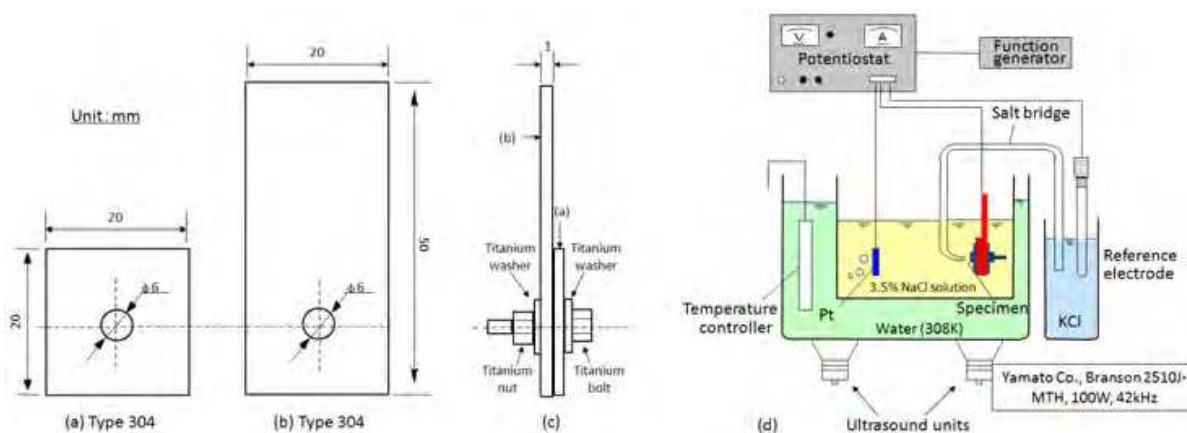


Fig. 5. (a-c) Specimen with crevice and (d) apparatus for polarization test. Copyright 2008 The Japan Institute of Metals

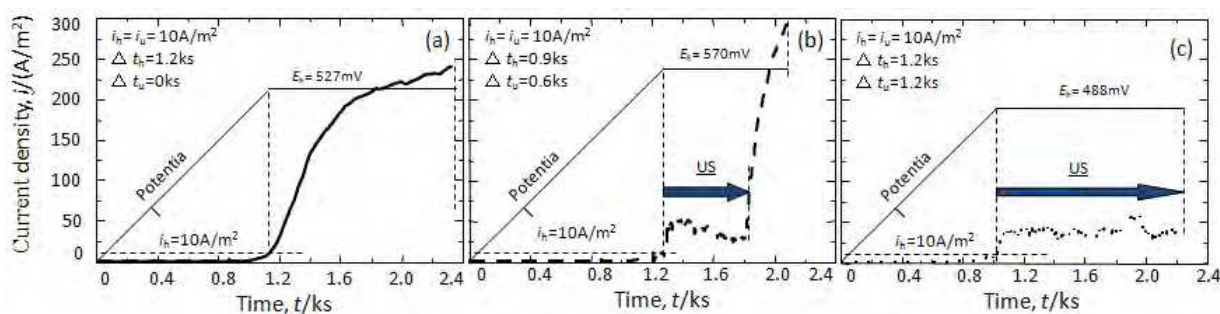


Fig. 6. Polarization curves without ultrasound (a), with ultrasound (b)  $i_h = i_u = 10$  A/m<sup>2</sup>,  $\Delta t_h = 0.9$  ks,  $\Delta t_u = 0.6$  ks, and with ultrasound (c)  $i_h = i_u = 10$  A/m<sup>2</sup>,  $\Delta t_h = 1.2$  ks,  $\Delta t_u = 1.2$  ks. Copyright 2008 The Japan Institute of Metals

Fig.7 shows the steel surface between crevices of (i) steel / steel and (ii) steel / washer (titanium) after the polarization. Crevice corrosion clearly appeared in any case. The difference between (a) and (b) is not remarkable probably because the applied period of ultrasound was short in (b), however, the corrosion area in (c) is clearly small.

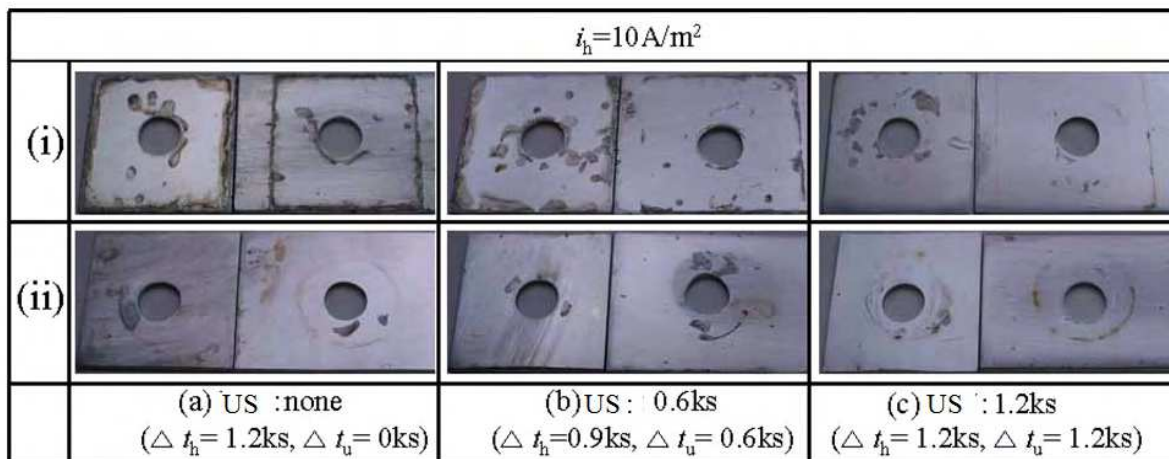


Fig. 7. Specimen surfaces after polarization without and with ultrasound ( $i_h = i_u = 10 \text{ A/m}^2$ ). Copyright 2008 The Japan Institute of Metals

Fig.8 shows the electric charge  $q$ , which is integrated with time during the period of potential holding for  $\Delta t_h = 0.6 \text{ ks}$ ,  $0.9 \text{ ks}$  or  $1.2 \text{ ks}$ . In the case of  $\Delta t_h = 0.6 \text{ ks}$ ,  $q$  without ultrasound was about  $65 \text{ kC/m}^2$ , however, it decreased to about  $15 \text{ kC/m}^2$  when the ultrasound was applied for  $0.6 \text{ ks}$ . In the case of  $\Delta t_h = 1.2 \text{ ks}$ ,  $q$  without ultrasound was about  $190 \text{ kC/m}^2$ , it decreased to about  $45 \text{ kC/m}^2$  when the ultrasound was applied for  $1.2 \text{ ks}$ . In addition, in the case of  $\Delta t_h = 0.9 \text{ ks}$  and  $\Delta t_u = 0.6 \text{ ks}$ ,  $q$  was about  $165 \text{ kC/m}^2$ . In any cases, about 77% of the electric charge decreased due to the application of ultrasound. Of course, the effect of ultrasound would be small if the ultrasound was midway stopped. The corrosion area of crevice corrosion is also shown in the right side of Fig.8 with hatching sticks. The corrosion area changed almost at the same ratio with the electric charge, although the depth of the corrosion zone would be different.

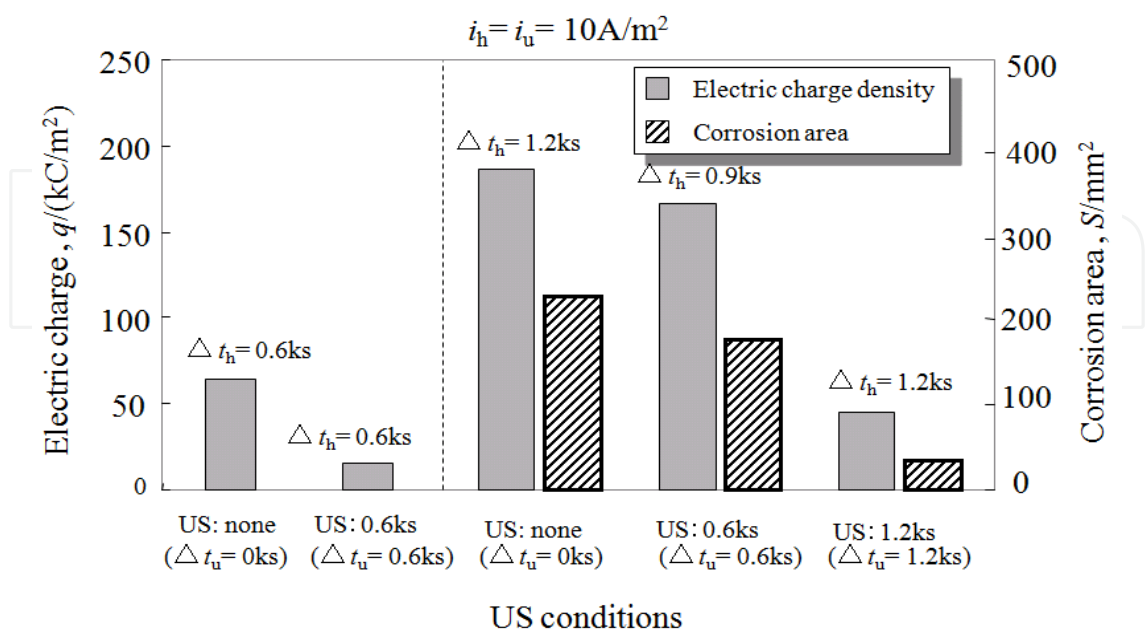


Fig. 8. Electric charge during the holding of potential without and with ultrasound ( $i_h = i_u = 10 \text{ A/m}^2$ ). Copyright 2008 The Japan Institute of Metals

Fig. 9 (a) shows the change of current density for another type of crevice specimen, where only one side of the specimen was polished when the potential was held constantly at  $i_h = 10 \text{ A/m}^2$ . On this specimen, both pitting corrosion (on the not polished side) and crevice corrosion occurred. After the current density reached  $i_u = 120 \text{ A/m}^2$  the ultrasound was applied for 60 s and then stopped for 60 s. Such ultrasound application / stop repeated for 4 cycles. In the first application of ultrasound, the current density largely decreased to about  $50 \text{ A/m}^2$ . It gradually recovered during the 60 s stop state of ultrasound to the previous level before the application of ultrasound. Such change almost synchronized with the cyclic application and stop of ultrasound. Fig.9 (b) shows the change of current density, after the current density reached  $i_h = 50 \text{ A/m}^2$  and the potential at that moment was kept constant. The ultrasound was applied for 60 s after the current density reached  $i_u = 250 \text{ A/m}^2$ , and then stopped for 270 s. Such ultrasound application was twice cycled. The current density can be largely decreased to about  $40 \text{ A/m}^2$  during the 60 s application of ultrasound. During the stop of ultrasound for 270 s, the current density gradually increased to the previous level. Almost the same change occurred in the second ultrasound cycle. According to the change of electric charge  $q$  calculated from Fig.9, either of the happening of pitting corrosion or crevice corrosion, the decrease in the corrosion amount by ultrasound was about 44~55% in comparison with those without ultrasound. Therefore, even if the ultrasound was not continuously applied, an intermittently application for 60 s can bring about large suppression of corrosion.

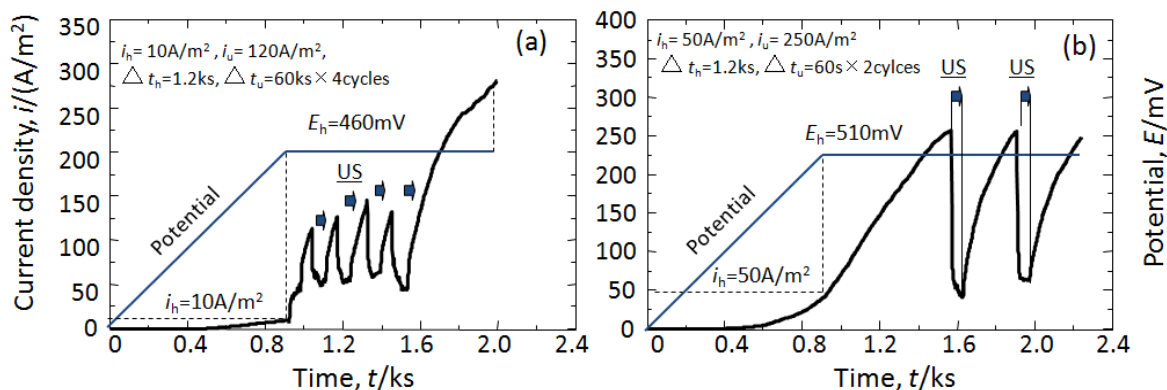


Fig. 9. Polarization curves of both pitting corrosion and crevice corrosion with ultrasound. (a):  $i_h = 10 \text{ A/m}^2$ ,  $i_u = 120 \text{ A/m}^2$ ,  $\Delta t_h = 1.2 \text{ ks}$ ,  $\Delta t_u = 60 \text{ s} \times 4 \text{ cycles}$ ; (b):  $i_h = 50 \text{ A/m}^2$ ,  $i_u = 250 \text{ A/m}^2$ ,  $\Delta t_h = 1.2 \text{ ks}$ ,  $\Delta t_u = 60 \text{ s} \times 2 \text{ cycles}$ . Copyright 2008 The Japan Institute of Metals

The schematic drawing of decrease in growth of crevice corrosion by application of ultrasound is shown in Fig.10. In the case of without ultrasound, the metallic ions ( $M^{n+}$ ) in the crevice will be accumulated by the flow of the passive current before crevice corrosion is triggered, and hydrogen ions increase due to the hydrolysis reaction of  $M^{n+}$ . Furthermore,  $Cl^-$  ions were attracted from solution out of the crevice to neutralize the excessive plus charge. Thus, the crevice corrosion is induced ((a)). That is,  $H^+$  and  $Cl^-$  ions enriched in the crevice with the anodic crevice corrosion and the corrosion is accelerated ((b), (c)). On the one hand, when the ultrasound was applied, the concentration of  $M^{n+}$ ,  $Cl^-$  and  $H^+$  inside the crevice can be diluted by the stirring effect of ultrasound, which results in the slowing down of the corrosion ((b'), (c')). In some cases, re-passivation of the crevice surface might occur (c). Of course, the promotion of the diffusion of oxygen into the crevice will also decrease the corrosion rate

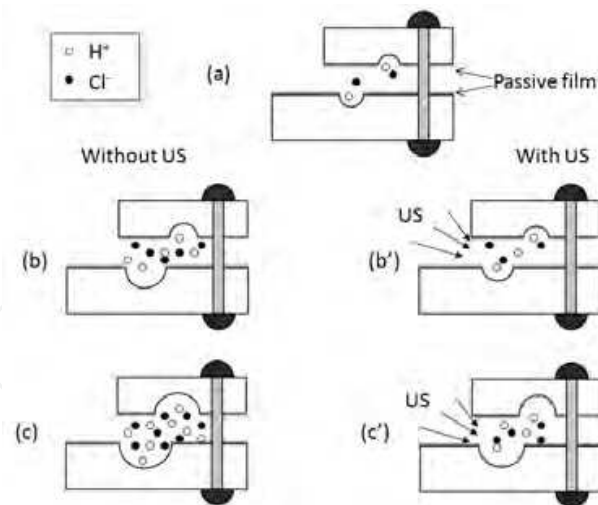


Fig. 10. Schematic drawing of decrease in growth of crevice corrosion by application of ultrasound. Copyright 2008 The Japan Institute of Metals

## 6. Influence of power and distance of ultrasound on pitting corrosion of Type 304 steel (Wang & Kido, 2009)

In this section, the influence of the transmitted acoustic power of ultrasound on the specimen and the vibrator-to-specimen distance on the pitting corrosion will be introduced. The corrosion tests were carried out in a corrosion cell connected to a potentiostat (Hokuto Denko Co., HAB-151) and an ultrasound vibrator (Kaijo Co., 4292C; 19.5kHz; 130 mm x 150 mm) (Fig.11). The input power to the ultrasound vibrator can be adjusted by a controller (Kaijo Co., TA-4021) from  $I = 0$  to  $I = 10$ , where the full input power of  $I = 10$  to vibrator is 200 W corresponding to a mean input intensity of 10 kW/m<sup>2</sup> from the vibrator. The specimen was immersed in 3.5% NaCl aqueous solution in the corrosion cell facing to the ultrasound vibrator and the temperature was tried to be kept stable at  $305 \pm 2$  K by an auto-heater (thermostat without cooling function), but the increased temperature in the solution was not further adjusted when ultrasound was applied.

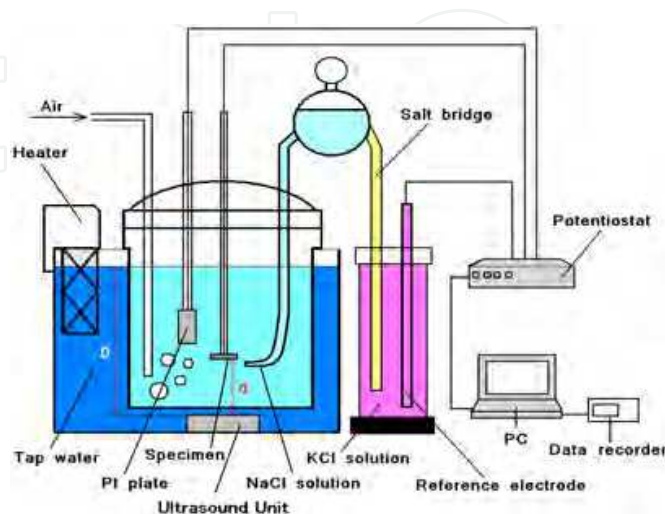


Fig. 11. Apparatus for polarization and applying ultrasound. Copyright 2009 Elsevier

The ultrasound was applied in simultaneously with the holding of potential. The distance from the ultrasound vibrator to the specimen surface ( $d$ ) and the input power to vibrator ( $I$ ) were changed as  $d = 76$  mm ( $I = 0, 2, 4, 6$  and  $8$ ) and  $I = 8$  ( $d = 19, 39, 76$  and  $95$  mm). Note that the wavelength ( $\lambda$ ) of the ultrasound in the frequency of 19 kHz is about 76 mm, which was calculated from the speed of sound of 1480 m/s. After the polarization tests, specimen surfaces were observed using an optical microscope and the corrosion areas were accordingly measured.

Fig.12 (a) shows the typical change of the current density in the pitting corrosion zone from  $i_h = 20$  A/m<sup>2</sup> during the period of simultaneously holding potential and applying ultrasound. The input power to ultrasound vibrator changed from  $I = 0$  to  $I = 8$  at a constant distance of  $d = 76$  mm. The distance is just equal to the wavelength of ultrasound in the solution. In Fig.12 (a), the anodic current density increased gradually with time during the period of holding potential without the application of ultrasound ( $I = 0$ ), however, the value largely decreased when the ultrasound was applied under each input power to vibrator. No large difference of the current density under  $I = 1, 2$  and  $4$  can be seen, but the current density sharply decreased under  $I = 6$ . The largest decrease of the current density was obtained when applying ultrasound under  $I = 8$  in this work. The smallest value of current density was near  $1 \times 10^{-3}$  A/m<sup>2</sup>, meaning the passivation of pits. Fig.12 (b) shows the electric charge obtained from the integrity of the current density during the potential holding. Each value of the electric charge is averaged from at least 3 tests. The value of electric charge was about 22 kC/m<sup>2</sup> without ultrasound ( $I = 0$ ), which is smaller than the value obtained in the previous report (Wang, 2008) perhaps because the chemical composition of the specimens in this work is different from those used in the previous work. The electric charge decreased to about 6 ~ 9 kC/m<sup>2</sup> when applying ultrasound under  $I = 1, 2$  or  $4$ . Large decrease in the electric charge was obtained under  $I = 6$  and  $I = 8$ , especially the electric charge under  $I = 8$  was the smallest one in this work (1 kC/m<sup>2</sup>). Such results gave the detail of the corrosion rate and meaning that the pitting corrosion of Type 304 stainless steel can surely be suppressed by the application of ultrasound in the solution and the suppression effect become remarkable with the increase in the input power to ultrasound vibrator.

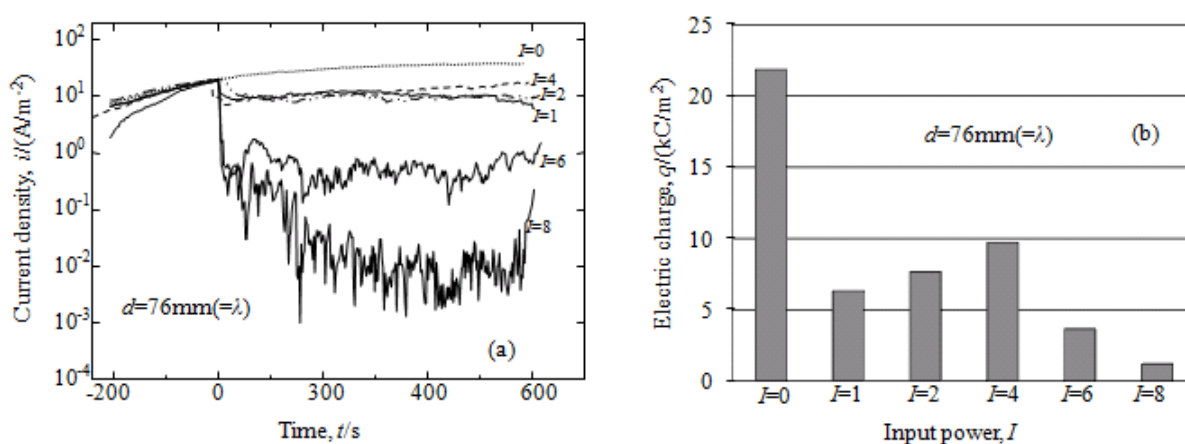


Fig. 12. Pitting current density (a) and accumulated electric charge (b) during the period of simultaneously holding potential and applying ultrasound with different input powers at a constant distance of 76 mm. Copyright 2009 Elsevier

Fig.13 (a) shows the surface morphology of specimens after the polarization tests in Fig.12. The area ratio and the mean depth of pits are shown in Fig.13 (b) and (c). The depth of pits was obtained by focusing on the bottom of pits and the flat specimen surface by moving an optical lens. Pits appeared on each specimen surface after the polarization, but the sum, size and depth gradually decreased with the increase in the input power to ultrasound vibrator. Although the difference of current density under  $I = 1, 2$  and  $4$  was indistinct, in Fig.13 it is known that the pitting corrosion can be suppressed more with the increase in the input power to ultrasound vibrator. The least and smallest pits were found when applying ultrasound under  $I = 8$ . It means that the initiation and growth of pits were suppressed both in the width and the depth by ultrasound.

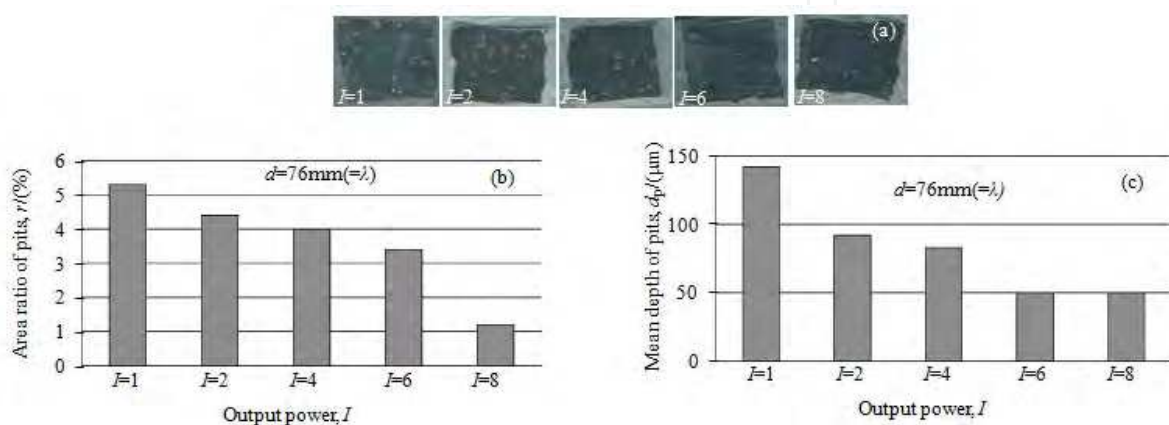


Fig. 13. Surface morphology (a), area ratio of pits (b) and mean depth of pits (c) on specimen surface after simultaneously holding potential and applying ultrasound with different input powers at a constant distance of 76 mm ( $=\lambda$ ). Copyright 2009 Elsevier

Fig. 14 (a) shows the pitting current density during the period of simultaneously holding potential and applying ultrasound at different distances under a constant input power of  $I = 8$  to vibrator. For each case with the application of ultrasound, the current density decreased by comparing to that without ultrasound. No large difference of the current density can be seen at the distance of  $d = 19$  and  $38$  mm, but the current density at  $d = 76$  mm was the smallest one while the current at  $d = 95$  mm was the largest one. Fig.14 (b) shows the electric charge during the potential holding under  $I = 2$  and  $8$  at different distances. According to the left part of Fig.14 (b) (averaged results under  $I = 2$ ), by comparing to that at  $d = 19$  mm ( $=\lambda/4$ ) the current density increased at  $d = 38$  mm ( $=\lambda/2$ ). However, it largely decreased at  $d = 76$  mm ( $=\lambda$ ). The current is the largest at the distance of  $d = 95$  mm ( $=5\lambda/4$ ). In the right side of Fig.14 (b) (averaged results under  $I = 8$ ), almost the same tendency was obtained with that under  $I = 2$ . Of course, the absolute value under  $I = 8$  is much smaller than that under  $I = 2$ .

Fig. 15 (a) shows the specimen surface after the corrosion test with changing the distance under  $I = 8$ . Fig.15 (b) and (c) show the area ratio and the mean depth of pits in these cases. It is clear that both the area ratio and the mean depth decreased with the increase of distance from  $d = 19$  mm to  $76$  mm, except the largest value appeared at the distance of  $d = 95$  mm. It suggests that the suppression effect of acoustic cavitation on the pitting corrosion depends not only on the distance but also on the transmission phase of the ultrasound wave. Larger suppression effect appears at the vibrator-to-specimen distance equals to the transmission wavelength of ultrasound.

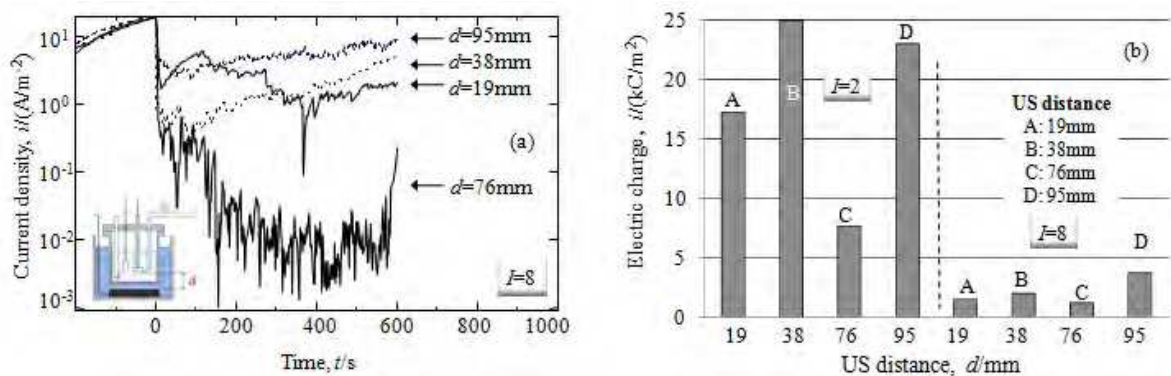


Fig. 14. Pitting current density (a) and accumulated electric charge (b) during the period of simultaneously holding potential and applying ultrasound with different distances at a constant input power of  $I = 8$  or  $I = 2$ . Copyright 2009 Elsevier

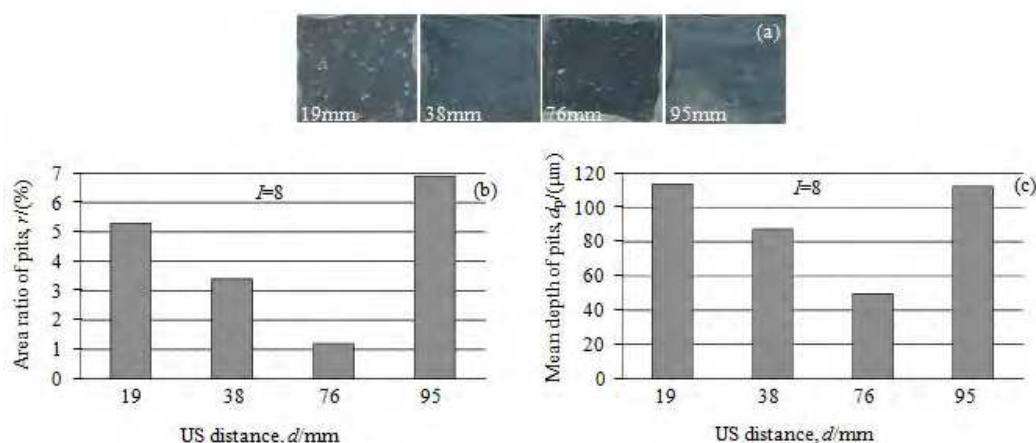


Fig. 15. Surface morphology (a), area ratio of pits (b) and mean depth of pits (c) on specimen surface after simultaneously holding potential and applying ultrasound with different distances at a constant input power of  $I = 8$ . Copyright 2009 Elsevier

Although the input power to ultrasound vibrator can be exactly set from the ultrasound controller (see Fig.11), the transmitted power dissipated near the specimen surface was not known. Here, the transmitted acoustic power near the specimen surface was measured by a calorimetry method as follows (CBHI, 1999; Whillock & Harvey, 1996). The temperature of 5 mL pure water contained in a small glass tube (inner diameter  $\phi = 12$  mm) was inserted into the water bath and measured at 10 s intervals by a digital thermometer during the sonication for a period of 120 s (before the application of ultrasound, the power of the auto-heater was cut). The absorbed acoustic power density ( $p$ ) was calculated using:

$$p = mC_p(dT / dt) / A \tag{1}$$

where  $m$  is the mass of water (unit: kg),  $C_p$  is the heat capacity of water (4180 J/(K · kg)) and  $dT/dt$  is the temperature rise per second during the initial 20 s (K/s),  $A$  is the cross-sectional area of the glass tube ( about 113 mm<sup>2</sup>). The result is shown in Fig.16. In Fig.16 (a), at the constant distance of  $d = 76$  mm, almost no temperature increase can be detected under the input power of  $I = 1$  and  $I = 2$  to vibrator, meaning the transmitted power is weak. In the case of  $I = 4$  the temperature slowly increased 0.4 K after 120 s, while the increased

temperatures are respectively 0.8 K and 1.6 K in the case of  $I = 6$  and  $I = 8$ . The above result shows the transmitted power of ultrasound to the specimen surface increases with the increase in the input power to vibrator. In each case of  $I = 4, 6$  and  $8$ , the temperature increased sharply at the initial 20 s but the increase became slow after then. This should be due to the happening of heat transfer in the solution during a relatively long period. Fig.16 (b) shows the temperature change under the constant input power of  $I = 8$  to vibrator with changing the distance from  $d = 19$  to 95 mm. In the case of  $d = 19$  mm and  $d = 95$  mm, the increase in temperature is almost the same after 120 s. This suggests that the transmitted power depends on the transmission phase of ultrasound wave. In the case of  $d = 38$  mm ( $= \lambda/2$ ), the temperature almost did not change at the initial 40 s but after then largely increased more than 2.8 K. In the case of  $d = 76$  mm, the largest increase of temperature obtained (more than 3.7 K). Note that two different curves of temperature are shown in Fig.16 (a) and (b) at the same condition of  $I = 8$  and  $d = 76$  mm.

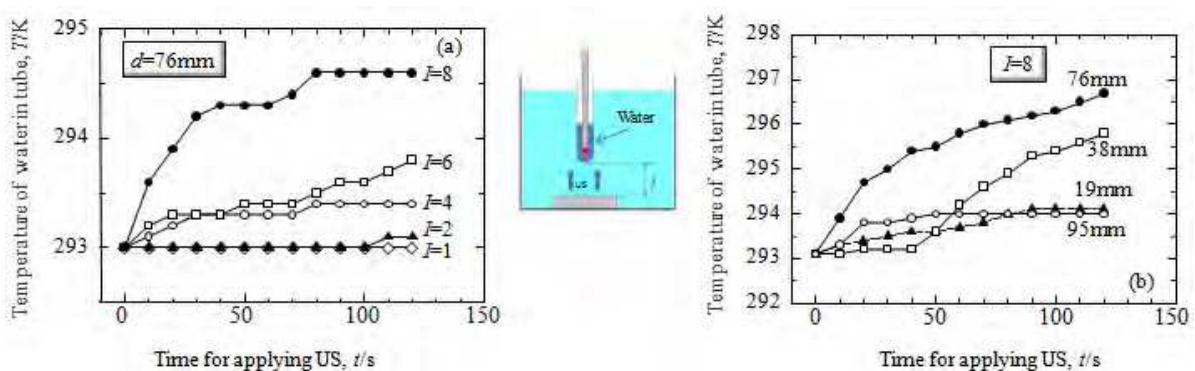


Fig. 16. Temperature change of a 5 mL pure water during the application of ultrasound in different cases. Copyright 2009 Elsevier

Table 1 shows the transmitted power of ultrasound near the specimen surface using the increase in temperature during the initial 20 s by equation 1). Comparing to the results in Fig.12~15, it is clear that the suppression effect on the pitting corrosion increased with the increase in the transmitted power of ultrasound. During a long period measurement, the increased temperature in the solution will also largely influence the corrosion rate. However, this would not change the conclusion of the suppression effect of ultrasound in the input power to the vibrator and the distance. It is clear that the transmitted power depends on both the input power to the vibrator and the ultrasound phase.

Fig.17 shows the change of current density when applying ultrasound in solutions with and without the addition of 0.5% ethanol at the constant distance of  $d = 76$  mm under the input power of  $I = 2$  and  $I = 8$  to vibrator. In the case of  $I = 2$ , the current density in the ethanol-added solution decreased comparing to that in the ethanol-not-added solution. This means that the enhanced cavitation in this solution enhanced the suppression effect on the pitting corrosion under a weak ultrasound. On the other hand, in the case of  $I = 8$ , the current in ethanol-added solution became larger and unstable comparing to that in the ethanol-not-added solution. (two curves in the ethanol-not-added solution were shown in Fig.17 (b), including the lowest and highest current in all measurements.) This means that the suppression effect of corrosion with the addition of ethanol decreased under higher input power to ultrasound vibrator.

Condition	$d=76$ (mm)					$I=8$			
	$I=1$	$I=2$	$I=4$	$I=6$	$I=8$	$d=19$ (mm)	$d=38$ (mm)	$d=76$ (mm)	$d=95$ (mm)
Increased temperature in 20 s (K)	-	-	0.2	0.3	0.9	0.4	0.2	1.7	0.8
Acoustic power density ( $\text{kJ/m}^2$ )	-	-	1.85	2.78	8.33	3.70	1.85	15.73	7.40

Table 1. Increased temperature and adsorbed acoustic power density in a 5 mL water when ultrasound is applied. Copyright 2009 Elsevier

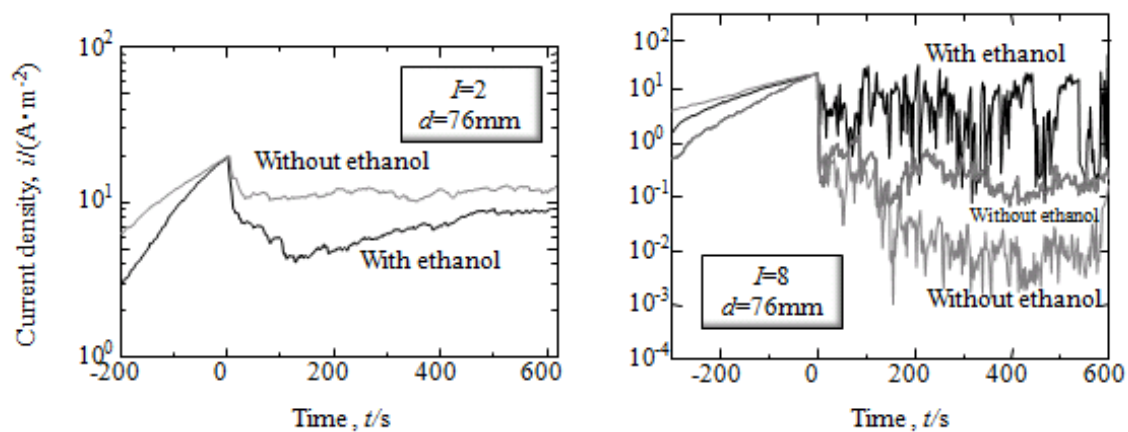


Fig. 17. Pitting current density during the period of simultaneously holding potential and applying ultrasound with different input powers at distance of  $d = 76$  mm and input power of  $I = 8$  in 3.5% NaCl solution containing 0.5% ethanol. Copyright 2009 Elsevier

When the acoustic cavitation is not strong enough to damage the passive film, the suppression effect of acoustic cavitation on pitting corrosion will increase with the increase in the stirring effect of solution in pits after removing the corrosion products (or the metallic cover). The suppression effect should be related to (1) the bubbles' size decided by the tensile stress and (2) the collapse power (shock wave power or cavitation power) decided by the compressive stress in the ultrasound field. Both of the stresses are determined by (i) the amplitude and (ii) the phase of the ultrasound wave. The collapse of larger bubbles brings about larger collapse power.

The removal of corrosion products or metallic covers can be promoted by larger collapse power of the cavitation under larger input power to vibrator and the solution in pits can be completely stirred. This is the reason that the suppression effect on corrosion can be enhanced when increasing the input power to vibrator from  $I = 1$  to  $I = 8$ . However, the stirring of solution in pits after removing corrosion products or metallic covers should depend on both the bubbles' size as well as the collapse power. The schematic drawing is shown in Fig.18. Note that not all the pits are covered by metallic covers (a). Near the specimen, micro-jets to the specimen surface will appear from each collapsing bubble. When the input power to vibrator is small the bubbles' size and the collapse power are small. Part of corrosion products will be cleaned out but no damage occurs on the metallic cover. However, the collapse of bubbles smaller than pits perhaps gives relatively effective stirring effect of solution in pits (b). With the increase in the input power to vibrator (c), the removal

of corrosion products increases but the metallic covers still remains there because of the strong strength connecting with the substrate. This results in that the stirring effect does not remarkably increase and thus the suppression effect on pitting corrosion did not largely increase when the input power to vibrator increased from  $I = 1$  to  $I = 2$  and  $I = 4$ . With further increase in the input power to ultrasound vibrator (d), the extremely enhanced cavitation power on the removal of corrosion products and metallic covers, and the stirring effect will be significantly enlarged (with the neglect of the weakness in the enlarged size of bubbles). That is the reason that the corrosion was greatly suppressed under  $I = 6$  and  $I = 8$ . Especially the current density decrease to a level of  $1 \times 10^{-3} \text{ A/m}^2$  under  $I = 8$ , meaning the growth of the pit almost stopped.

On the other hand, the transmitted power to the specimen generally decreases with the increase in the vibrator-to-specimen distance because of the amplitude attenuation of ultrasound wave. It resulted in the decrease in the suppression effect when increasing the distance from  $d = 19 \text{ mm}$  to  $d = 38 \text{ mm}$  and  $d = 95 \text{ mm}$ . On the other hand, the phase change of the wave should be also considered in the explanation of the result. In this section, the largest suppression effect of pitting corrosion was obtained at a distance of  $d = 76 \text{ mm}$ , which is just equal to wavelength of ultrasound in the solution. In another word, the phase of the wave there is the same with that on the vibrator surface. This should be related to the formation of a "standing wave field" of ultrasound in the solution with overlapping the forward wave from the vibrator and the backward (reflected) wave from the liquid / air surface (CBHI, 1999; Mitome, 2008). In the standing wave field, anti-nodes with strong cavitation generally appears with an interval of  $\lambda/2$  along the transmission direction. However, in this work only at a distance of  $\lambda$  (76 mm) the suppression effect of pitting corrosion is large while the suppression effect at a distance of  $\lambda/2$  is much small (with good correspondence to the temperature measurement). The reason has not been clearly know, perhaps due to the unfixed distance from the vibrator to the solution surface in the above measurement.

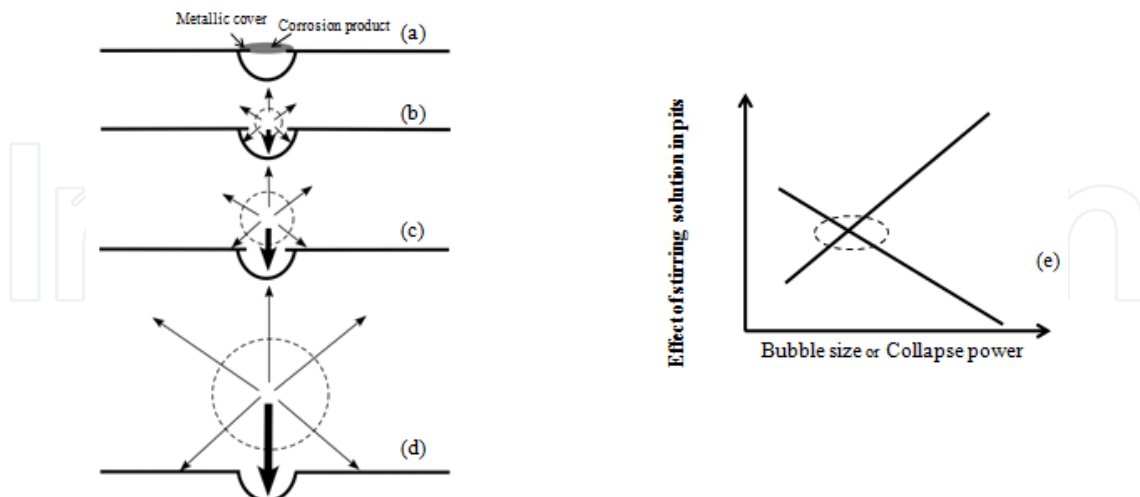


Fig. 18. Schematic drawing of relation of effect of stirring solution in pits with change of bubble size and collapse power. (a) Pit is covered by metallic cover and corrosion product; (b) corrosion product is removed by smaller collapsing bubble; (c) (d) corrosion product and metallic cover is removed by larger collapsing bubble; (e) stirring effect and bubble size or collapse power. Copyright 2009 Elsevier

Except the amplitude of ultrasound, the power of cavitation is also influenced by the evaporability of solution (CBHI, 1999). Ethanol is evaporable specie to improve the evaporability of the solution to result in the increase in stronger cavitation. Accordingly, the corrosion behaviour of stainless steel in the ethanol-added solution changed much with the application of ultrasound. In the case of  $I = 2$ , the current density is smaller in the ethanol-added solution than that in the ethanol-not-added solution. This means that the improved cavitation in ethanol-added solution gave fully stirring of the solution in the pits and suppressed the growth of pits. On the other hand, in the case of  $I = 8$ , the suppression of corrosion became weak after adding ethanol in the solution. This should be due to the activation of passive films on the surface by the excessively enhanced cavitation, which bring about promotion of pitting corrosion. This also means that strong acoustic cavitation can also promote corrosion, which corresponds well with other reports described before.

### 7. Influence of frequency of ultrasound on the pitting corrosion of Type 304 steel (Wang, 2011)

The influence of the ultrasound frequency as well as the distance from vibrator to specimen on the growth of pitting corrosion will be introduced in this section. The vibrators were used with different frequencies of  $f_1 = 19.5$  kHz (Vibrator: Kaijo Co., 4292C),  $f_2 = 50$  kHz (4492H) or  $f_3 = 420$  kHz (4711C). The input power to the ultrasound vibrator was set at  $I = 8$  by a controller (Kaijo Co., TA-4021). The distance from the vibrator to the specimen ( $d$ ) was varied with the wavelength of each type of ultrasound ( $\lambda_1 = 76$  mm,  $\lambda_2 = 29.6$  mm,  $\lambda_3 = 3.5$  mm). In addition, the distance ( $D$ ) from vibrator to the solution surface was set as several integral times of the half-wavelength of each ultrasound, i.e.,  $1.5 \lambda_1$  ( $D_1 = 114$  mm),  $3 \lambda_2$  ( $D_2 = 89$  mm) or  $27.5 \lambda_3$  ( $D_3 = 96$  mm). Note that the distance of  $D$  from vibrator to the solution surface in the above sections was not precisely fixed; only in this section the *standing wave* from the solution surface can be discussed. When the anodic current density reached the value of  $i_h = 20$  A/m<sup>2</sup> in the pitting growth zone, the potential was immediately held constant for 600 s. The ultrasound was applied simultaneously with the holding of potential for 600 s.

Fig.19 (a) shows the accumulated electric charge during the period of simultaneously holding potential and applying ultrasound at  $I = 8$  with different frequencies (a: 19.5 kHz; b: 50 kHz; c: 420 kHz) and different vibrator-to-specimen distances. Although the input powers to the vibrators are the same, the suppression effects on the pitting corrosion showed large difference when changing either the frequency or the vibrator-to-specimen distance. At each frequency, there is an optimum distance where the largest suppression effect was obtained. The optimum vibrator-to-specimen distance is respectively 57 mm ( $= 3\lambda_1/4$ ) in the case of  $f_1 = 19.5$  kHz, 29.6 mm ( $= \lambda_2$ ) in the case of  $f_2 = 50$  kHz, and 17.6 mm ( $= 5 \lambda_3$ ) in the case of  $f_3 = 420$  kHz. This difference should be attributed to the balance of the formation of standing wave and the energy attenuation of ultrasound in the solution. In addition, the suppression effect in the case of 19.5 kHz is much larger than (100 times of) those in the cases of 50 kHz and 420 kHz. The latter two effects are almost the same.

From the observation of specimen surfaces after the polarization, the area ratio and the mean depth of pits are obtained (Fig.19 (b, c)). Note that the values were obtained from the surfaces after further ultrasonically cleaning with multi-vibrators (Fig.2). Pits appeared on each surface after the polarization and the pitting corrosion was surely suppressed by each type of ultrasound. However, the suppression of corrosion does not directly decrease the sum of pits. In several different distances of 19.5 kHz and 420 kHz the sum did not decrease, while in the

case of 50 kHz the sum increased reversely in comparison with that without ultrasound. On the other hand, the total area of pits (Fig.19 (b)) changed, corresponding well with that of the accumulated electric charge for all ultrasound conditions. Large difference cannot be found in the depth of pits under different ultrasound conditions (Fig.19 (c)). The pits in the case of 50 kHz looked like a little shallower than others. This should be attributed to the low precision of the dial gauge (minimum value: 0.01 mm) and attribute to the residual metallic covers on pits (Laycock et al., 1998) (see description later in Fig.21 and 22). In general, the depth of pits with ultrasound is much shallower than those without ultrasound.

Fig.19 (d) shows the cavitation power during applying ultrasound with different frequencies and distances from the vibrator. According to the former report (Wang & Kido, 2009) , at the frequency of 19.5 kHz and at the distance of 76 mm, the cavitation power kept increasing with the increase in the input power from  $I = 0$  to 8. In this work, at the frequency of 19.5 kHz and the input power of  $I = 8$ , the cavitation power kept increasing with the increase in the distance from 19 mm and reached the maximum value of about  $9.5 \text{ kJ}/(\text{m}^2 \cdot \text{s})$  at the distance of  $d = 57 \text{ mm}$ . However, the power decreased with further increasing the distance and obtained the value of  $2.2 \text{ kJ}/(\text{m}^2 \cdot \text{s})$  at  $d = 95 \text{ mm}$ . The largest cavitation power at  $d = 57 \text{ mm}$  corresponds to the largest suppression effect on the growth of pitting at this frequency. On the other hand, the cavitation power at the frequency of 50 kHz did not show large change from the distance of 14.8 mm to 59.2 mm, which also corresponds well to the not largely changed suppression effect on pitting corrosion in this case. In the case of 420 kHz, the cavitation power at 17.6 mm and 35.2 mm was almost the same and that at 70.4 mm became a little small. This corresponds to the suppression effect on corrosion, where the largest effect was obtained at 17.6 mm in this case. On the other hand, the power at 50 kHz was the largest, with about 7~35 times of that of 19.5 kHz and 420 kHz. The power at 420 kHz was the smallest.

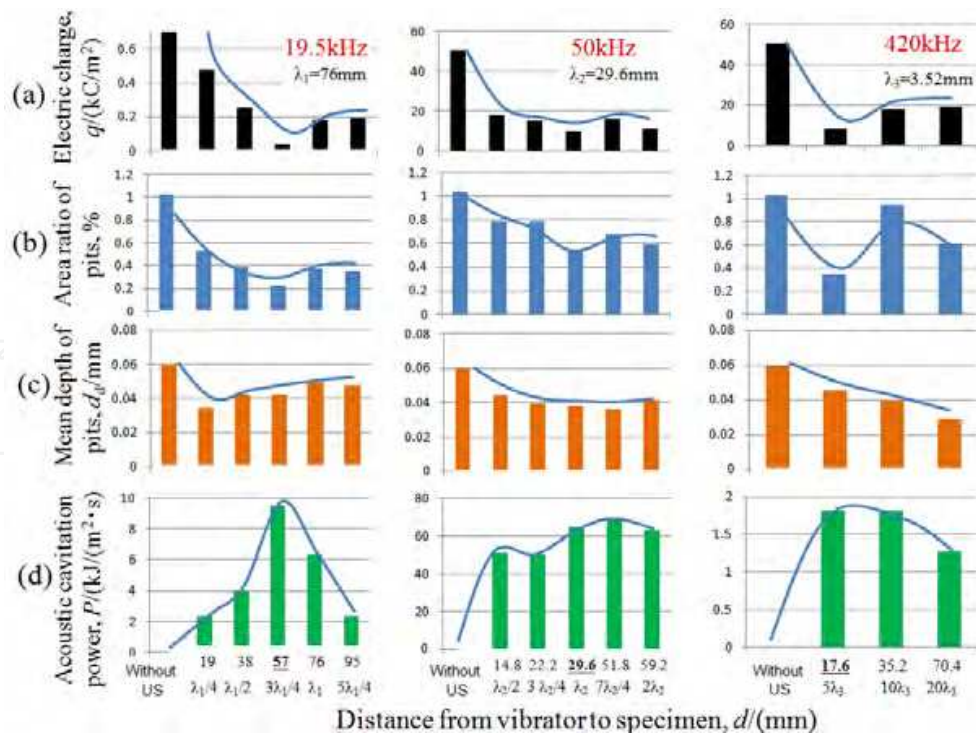


Fig. 19. Electric charge during potential holding and ultrasound applying (a), pit area ratio (b), pit depth (c) after polarization and cavitation power (d) during ultrasound applying. Copyright 2011 Japan Society of Corrosion Engineering

It is known as above that the suppression effect on the pitting corrosion increased with the increase in the cavitation power when the power is less than  $10 \text{ kJ}/(\text{m}^2 \cdot \text{s})$  in the case of 19.5 kHz and 420 kHz. The optimum condition to suppress corrosion appeared at 19.5 kHz at the distance of 57 mm. However, when the cavitation power is larger than  $50 \text{ kJ}/(\text{m}^2 \cdot \text{s})$  in the case of 50 kHz, the much large cavitation power is not helpful to increase the suppression effect. This result should be attributed to the simultaneous damage of the passive film on the specimen surface. Of course, during a long period measurement, the increased temperature in the solution will also influence the corrosion rate to some extent. That is, the transmission power depends on both the input power to vibrator and the ultrasound wave phase.

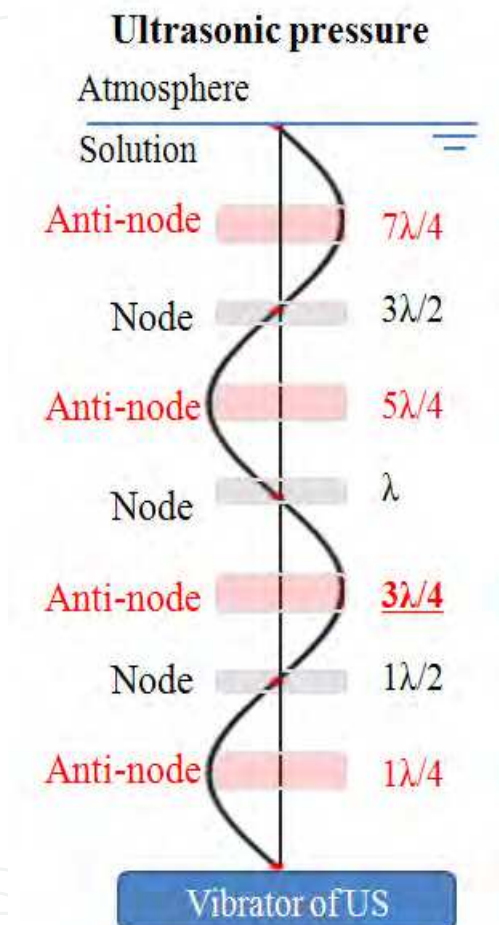


Fig. 20. Standing wave of ultrasonic pressure ultrasound from the vibrator to the solution surface. The large ultrasonic pressure generally appears at anti-nodes.

Fig.20 shows the simulated standing wave of ultrasonic pressure in the solution from the vibrator to the solution surface. Since the distance between the vibrator and the solution surface is set as several times of the half-wavelength of ultrasound, the large ultrasonic pressure generally appears at positions from either the solution surface or the vibrator surface with the interval of half-wavelength. Such positions of  $\lambda/4$ ,  $3\lambda/4$ ,  $5\lambda/4$  and  $7\lambda/4$  from the vibrator are called as anti-nodes, where large cavitation theoretically occurs. This can be used to well explain the largest cavitation power and the largest suppression effect of corrosion at the  $3\lambda_1/4$  in the case of 19.5 kHz. However, large cavitation power and suppression effect did not appear at other anti-nodes, which should also be influenced by

the energy attenuation of ultrasound in the solution. In the case of 50 kHz and 420 kHz, large cavitation power and suppression did not obtain at either of anti-nodes. In the case of 420 kHz, the wavelength is too small to precisely discuss the influence of position.

In the case of 19.5 kHz, the suppression effect of corrosion increased with the increase in the cavitation power when the power is less than  $10 \text{ kJ}/(\text{m}^2 \cdot \text{s})$ . The effect should be attributed to the increased stirring effect of solution in pits after removing the corrosion products and the metallic covers. The cavitation power is generally related to the bubbles' size decided by the tensile stress and the sum of the collapsed bubbles. In general, the bubble size becomes smaller with the increase in the frequency of ultrasound and thus the happening of cavitation becomes difficult. This should be the reason to get the small cavitation power in the case of 420 kHz, which brought about weak suppression effect of corrosion. On the other hand, the much large cavitation power in the case of 50 kHz should be attributed to the increased sum of collapse of bubbles rather than the balance of the decreased bubbles' size.

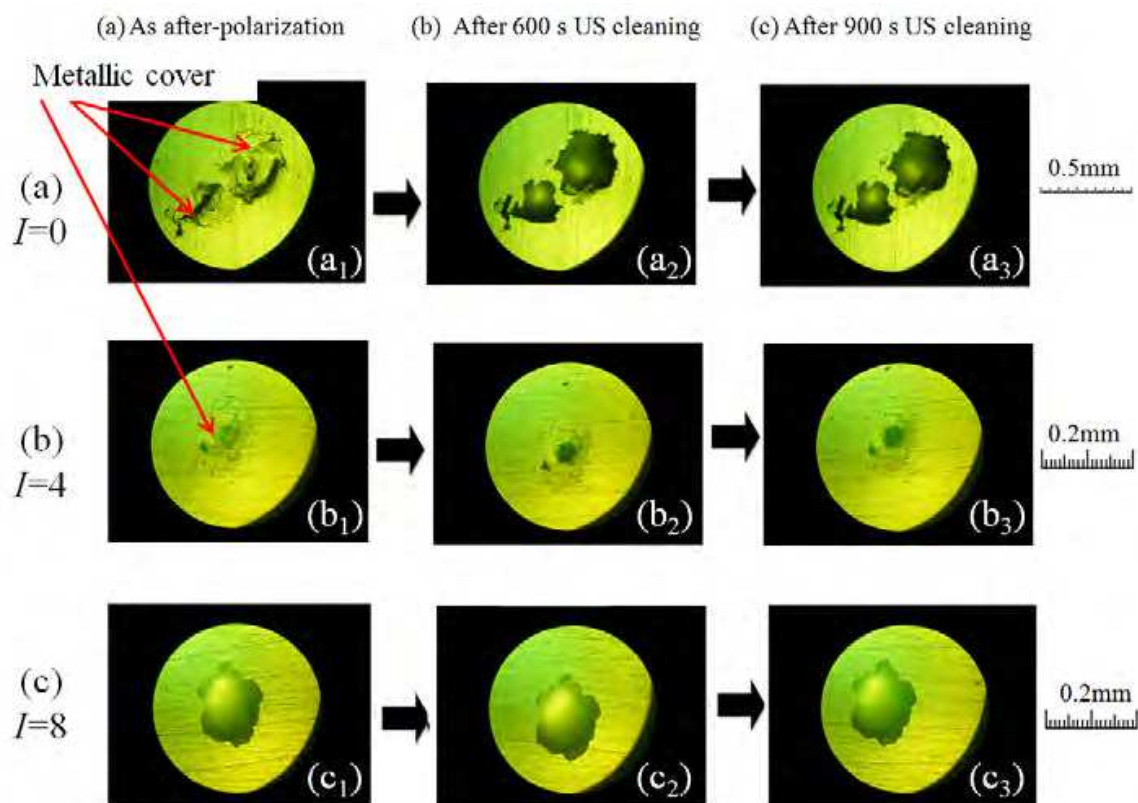


Fig. 21. Surface morphology of specimens after simultaneously holding potential and applying ultrasound at  $I = 0$  (a),  $I = 4$  (b) and  $I = 8$  (c) at frequency of 19.5 kHz. The surfaces  $a_1$ ,  $b_1$  and  $c_1$  are cleaned only by running distilled water;  $a_2$ ,  $b_2$ ,  $c_2$  and  $a_3$ ,  $b_3$ ,  $c_3$  are further cleaned in distilled water by an ultrasound cleaner for a total time of 600 s and 900 s.

Fig. 21 shows the specimen surfaces after the polarization with ultrasound at  $I = 0$ , 4 and 8 at the frequency of 19.5 kHz. The surfaces ( $a_1$ ,  $b_1$ ,  $c_1$ ) are rinsed only by running distilled water, while the surfaces ( $a_2$ ,  $b_2$ ,  $c_2$  and  $a_3$ ,  $b_3$ ,  $c_3$ ) are further cleaned in distilled water in an ultrasound cleaner with multi-vibrators (Fig.1) for 600 s or 900 s. Corrosion products were not found on the specimen without ultrasound (a), indicating that not all corrosion products reside on pits during the corrosion process. On the other hand, the metallic cover was left on

the pits when ultrasound was applied at  $I = 0$  and 4 (a, b), while it disappeared at  $I = 8$ . This means that the metallic cover forms during the corrosion and they can be removed when the applied ultrasound power is strong enough. Such removal of metallic cover and corrosion products is the reason of the suppression of the pitting corrosion. The depth of pit after further ultrasound cleaning was measured again and the results were shown in Fig.22. Of course the mean depth became larger than that before the ultrasound clean, which surely decreased with the increase in the input power from  $I = 0$  to 8 but didn't verify much with the change of vibrator-to-specimen distance.

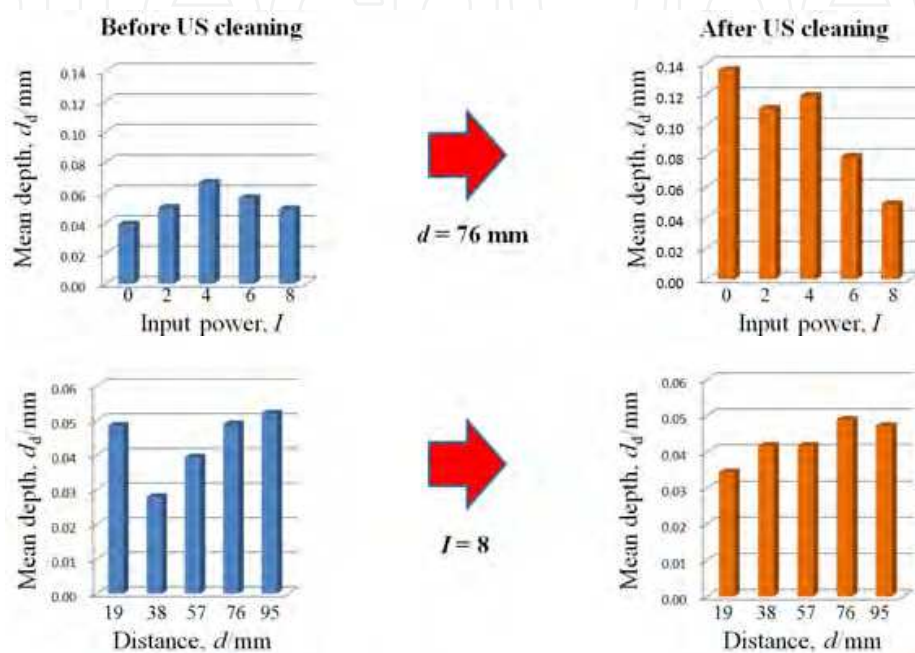


Fig. 22. Mean depth of pits before and after ultrasound cleaning on specimens, which were polarized by simultaneously holding potential and applying ultrasound with frequency of  $f_1 = 19.5$  kHz.

Fig. 23 shows the re-passivation behaviour of the specimen when the potential was swift back from 500 mV at 19.5 kHz and  $d = 57$  mm. In the case of without ultrasound (a), the re-passive potential appeared at -93 mV with a necessary accumulated charge of 218 kC/m<sup>2</sup>, while the potential became 316 mV with only a much smaller charge of 1 kC/m<sup>2</sup>. This promoted re-passivation behaviour by ultrasound is attributed to the remove of corrosion products and the metallic cover with the disturbing of the solution in pits.

## 8. Future works

According to the above results, it is clear that the pitting corrosion can be suppressed by either type of ultrasound. However, the influence on the initiation of pits has not been known, which will be investigated in the near future. Except the above physical effect of ultrasound application in solution, a chemical effect should also be considered. When the ultrasound is applied to an aqueous solution, water can be decomposed to  $H \cdot$  and  $OH \cdot$  radicals, and the solution becomes weak acidic (Jana & Chatterjee, 1995). According to the report of Jana, about  $3 \times 10^{21} / m^3$  radicals are produced by the ultrasound (frequency: 20 kHz, intensity: 190 k W/m<sup>2</sup>) and four  $OH \cdot$  transfer one  $Fe^{2+}$  ion to one  $Fe^{3+}$ . The ultrasound

intensity in this research was about 3~10 kW/m<sup>2</sup>, and the application time is short. Therefore, the amount of radicals produced will be not large. However, it is possible that there is a contrary influence of radicals on the pitting corrosion behaviour considering the breakdown of passive film by lowered pH solution by H • radical and the re-passivation of the broken passive film by the OH • radical with strong oxidation ability.

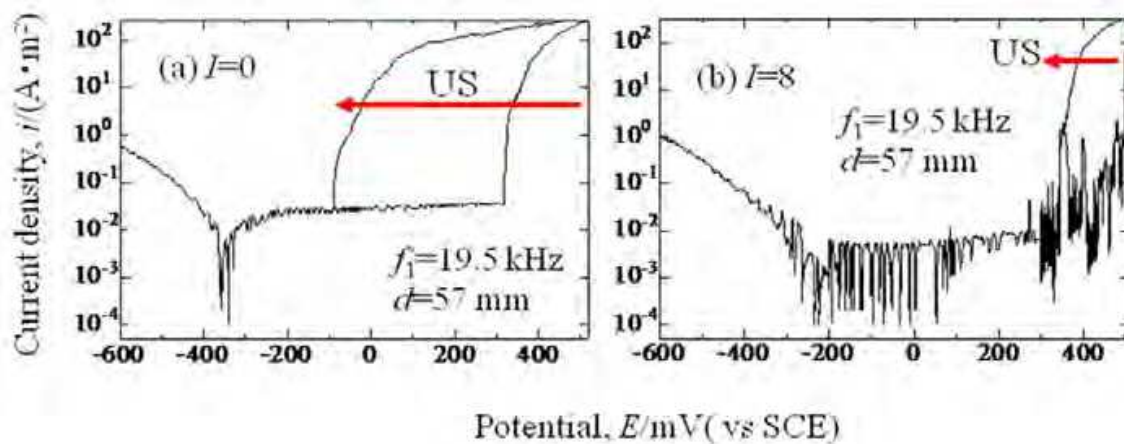


Fig. 23. Polarization curves with reversely sweeping of the potential at 500 mV, simultaneously without or with ultrasound with  $f_1 = 19.5$  kHz at  $d = 57$  mm and  $I = 8$ .

## 9. Conclusions

The influence of ultrasound in solution on the corrosion behaviour of stainless steel was introduced basing on our results and other literatures. It has known that when the acoustic cavitation caused by ultrasound is strong enough, the passive film can be damaged and thus corrosion is activated. However, when the acoustic cavitation caused by ultrasound is not strong enough to damage the passive film the corrosion will not be accelerated. As for the suppression effect of ultrasound on the stainless steel of Type 304 stainless steel, the following conclusions were obtained.

1. In case of pitting corrosion of Type 304 steel, the corrosion product was in-situ confirmed on the growing pits at the early stage. When the corrosion product was removed by the probe of AFM, the growth rate of pits largely decreased, which was explained by the decrease in the concentration of chloride and hydrogen ions in pits.
2. The cathode current, passive current and corrosion potential in the polarization curve were not almost changed by the application of ultrasound. However, the growth of pitting corrosion and crevice corrosion of Type 304 stainless steel can be suppressed by ultrasound with 19.5 kHz ultrasound. The change of the current density almost synchronized with the cyclic application and stop of ultrasound. In the case of 19.5 kHz at a constant vibrator-to-specimen distance of  $d = 76$  mm, the suppression effect on pitting corrosion increased with the input power to vibrator.
3. The suppression effect of the growth of pitting corrosion was different when changing either the frequency or the distance from ultrasound vibrator to the specimen with either of frequencies of 19.5, 50 and 420 kHz. The largest suppression effect in this work was obtained at 19.5 kHz at the vibrator-to-specimen distance of 57 mm at the input power of  $I = 8$  to vibrator.

4. The suppression effect of the growth of pitting corrosion became large with the increase in the cavitation power when the power is less than 10 kJ/(m<sup>2</sup>·s). However, in the case of 50 kHz, the cavitation was strong enough to damage the passive film, which weakens the suppression effect on the corrosion. In the case of 420 kHz, the effect on the suppression of corrosion was weak due to small cavitation power.
5. The ultrasound promotes the re-passivation of pits by not only removing corrosion products but also removing the metallic cover.

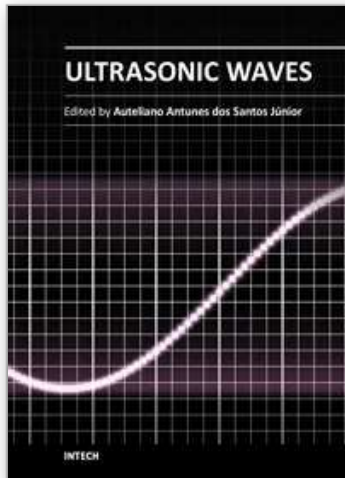
## 10. Acknowledgment

This work is a summary of our recent researches on *suppression of corrosion of stainless steel by ultrasound*, which were carried out in Hiroshima University (2004.4~2005.3) and in Hiroshima Institute of Technology (2005.4~2011.7). Professor K.Nakasa gave important advices and discussion in this work. Dr. Q.Zhang helped the in-situ observation of pitting corrosion by atomic force microscope. The author is very grateful to Mr. T.Tamai, Mr. A.Yamamoto, Mr. T.Kangai, Mr. H.Morishita, Mr. S.Nagai, Mr.Y.Odagami, Mr. K.Etsuki, Mr. M.Kimura, Mr. H.Do, Mr. G.Nishida, Mr. Y.Shibatani and Mr. S.Fujii for their assistance of experiments. Part of this work was supported by MEXT.HAITEKU, 2004~.

## 11. References

- Ryan, M.P.; Williams, D.E.; Chater, R.J.; Hutton, B.M. & Mcphail, D.S. (2002). Why stainless steel corrodes. *Nature*, Vol.415, No.6873, (February 2002), pp.770-774, ISSN 0028-0836
- Shimizu, K. (2010). New Role of a Low-Voltage, Ultra-High Resolution FE-SEM for Corrosion Studies (2) - Application examples -. *Zairyo-to-Kankyo / Corrosion Engineering of Japan*, Vol.59, No.7, (July 2010), pp.245-250, ISSN 0917-0480
- Shimizu, K. (2010). New Role of a Low-Voltage, Ultra-High Resolution FE-SEM for Corrosion Studies (1) - Sample Surface Preparation for Ultra-High Resolution FE-SEM -. *Zairyo-to-Kankyo / Corrosion Engineering of Japan*, Vol.59, No.10, (October 2010), pp.360-365, ISSN 0917-0480
- Yashiro, H. & Shimizu, K. (2010). *Poc. 57th Japan Conf. Materials and Environments, JSCE*, pp.175-178
- Hisamatsu, Y. (1981). Localized Corrosion of Iron-Nickel-Chromium Alloys - Pitting, Crevice Corrosion, and Stress Corrosion Cracking -. *Bulletin of the Japan Institute of Metals*, Vol.20, No.1, (1981), pp.3-11, ISSN 1340-2625
- Zhang, Q.; Wang, R.; Kato, M. & Nakasa, K. (2005). Observation by atomic force microscope of corrosion product during pitting corrosion on SUS304 stainless steel. *Scripta Materialia*, Vol.52, No.3, (February 2005), pp.227-230, ISSN 1359-6462
- Wang, R. & Kido, M. (2009). Influence of input power to vibrator and vibrator-to-specimen distance of ultrasound on pitting corrosion of SUS304 stainless steel in 3.5% chloride sodium aqueous solution. *Corrosion Science*, Vol.51, No.8, (August 2009), pp.1604-1610, ISSN 0010-938X
- Chouonpa Binran Henshu Iinkai (1999). *Hand Book of Ultrasonic Wave*, Maruzen, ISBN 4-621-04663-0 C 3055

- Alkire, R.C. & Perusich, S. (1983). The effect of focused ultrasound on the electrochemical passivity of iron in sulfuric acid. *Corrosion Science*, Vol.23, No.10, (October 1983), pp.1121-1132, ISSN 0010-938X
- Al-Hashem, A.; Caceres, P.G.; Riad, W.T. & Shalaby, H.M. (1995). Cavitation corrosion behavior of cast nickel-aluminum bronze in seawater. *Corrosion*, Vol.51, No.5, (May 1995), pp.331-342, ISSN 0010-9312
- Whillock, G.O.H. & Harvey, B.F. (1996). Preliminary investigation of the ultrasonically enhanced corrosion of stainless steel in the nitric/chloride system. *Ultrasonics Sonochemistry*, Vol.3, No.2, (1996), pp. S111-S118, ISSN 1350-4177
- Kwok, C.T.; Cheng, F.T. & Man, H.C. (2000). Synergistic effect of cavitation erosion and corrosion of various engineering alloys in 3.5% NaCl solution. *Materials Science Engineering A*, Vol.290, No.1-2, (October 2000), pp.145-154, ISSN 0921-5093
- Whillock, G.O.H. & Harvey, B.F. (1997). Ultrasonically enhanced corrosion of 304L stainless steel II: the effect of frequency, acoustic power and vibrator-to specimen distance. *Ultrasonics Sonochemistry*, Vol.4, No.1, (January 1997), pp.33-38, ISSN 1350-4177
- Nakayama, T. & Sasa, K. (1976). Effect of ultrasonic waves on the pitting potential of 18-8 stainless steel in sodium chloride solution. *Corrosion*, Vol.32, No.7, (July 1976), pp.283-285, ISSN 0010-9312
- Wang, R. & Nakasa, K. (2007). Effect of ultrasonic wave on the growth of corrosion pits on SUS304 stainless steel. *Materials Transactions*, Vol.48, No.5, (May 2007), pp.1017-1022, ISSN 1345-9678
- Wang, R. & Kido, M. (2008). Influence of application of ultrasound on corrosion behavior of SUS304 stainless steel with crevice. *Materials Transactions*, Vol.49, No.8, (August 2008), pp.1806-1811, ISSN 1345-9678
- Wang, R. (2008). Influence of ultrasound on pitting corrosion and crevice corrosion of SUS304 stainless steel in chloride sodium aqueous solution. *Corrosion Science*, Vol.50, No.2, (February 2008), pp.325-328, ISSN 0010-938X
- Wang, R. (2011). Growth behavior of pitting corrosion of SUS304 stainless steel in NaCl aqueous solution when applying ultrasound with different frequencies. *Zairyo-to-Kankyo / Corrosion Engineering of Japan*, Vol.60, No.2, (February 2011), pp.66-68, ISSN 0917-0480
- Wranglen, G. (1985). *An Introduction to Corrosion and Protection of Metals*. Chapman and Hall, ISBN 0412260409
- Japanese Industrial Standards Committee (2002). *JIS G0592:2002, Method of determining the repassivation potential for crevice corrosion of stainless steels*
- Mitome, H. (2008). Generation of acoustic cavitation and its application. *Journal of the Japan Society of Mechanical Engineering*, Vol.111, No.1074, (May 2008), pp.32-35, ISSN 0021-4728
- Laycock, N.J.; White, S.P.; Noh, J.S.; Wilson, P.T. & Newman, R.C. (1998). Perforated covers for propagating pits. *Journal of the electrochemical society*, Vol.145, No.4, (April 1998), pp.1101-1108, ISSN 0013-4651
- Jana, A.K. & Chatterjee, S.N. (1995). *Ultrasonics Sonochemistry*, Vol.2, No.2, (1995), pp.s87-s91, ISSN 1350-4177



## **Ultrasonic Waves**

Edited by Dr Santos

ISBN 978-953-51-0201-4

Hard cover, 282 pages

**Publisher** InTech

**Published online** 07, March, 2012

**Published in print edition** March, 2012

Ultrasonic waves are well-known for their broad range of applications. They can be employed in various fields of knowledge such as medicine, engineering, physics, biology, materials etc. A characteristic presented in all applications is the simplicity of the instrumentation involved, even knowing that the methods are mostly very complex, sometimes requiring analytical and numerical developments. This book presents a number of state-of-the-art applications of ultrasonic waves, developed by the main researchers in their scientific fields from all around the world. Phased array modelling, ultrasonic thrusters, positioning systems, tomography, projection, gas hydrate bearing sediments and Doppler Velocimetry are some of the topics discussed, which, together with materials characterization, mining, corrosion, and gas removal by ultrasonic techniques, form an exciting set of updated knowledge. Theoretical advances on ultrasonic waves analysis are presented in every chapter, especially in those about modelling the generation and propagation of waves, and the influence of Goldberg's number on approximation for finite amplitude acoustic waves. Readers will find this book a valuable source of information where authors describe their works in a clear way, basing them on relevant bibliographic references and actual challenges of their field of study.

### **How to reference**

In order to correctly reference this scholarly work, feel free to copy and paste the following:

Rongguang Wang (2012). Suppression of Corrosion Growth of Stainless Steel by Ultrasound, Ultrasonic Waves, Dr Santos (Ed.), ISBN: 978-953-51-0201-4, InTech, Available from:

<http://www.intechopen.com/books/ultrasonic-waves/suppression-of-corrosion-growth-of-stainless-steel-by-ultrasound>

**INTECH**  
open science | open minds

### **InTech Europe**

University Campus STeP Ri  
Slavka Krautzeka 83/A  
51000 Rijeka, Croatia  
Phone: +385 (51) 770 447  
Fax: +385 (51) 686 166  
[www.intechopen.com](http://www.intechopen.com)

### **InTech China**

Unit 405, Office Block, Hotel Equatorial Shanghai  
No.65, Yan An Road (West), Shanghai, 200040, China  
中国上海市延安西路65号上海国际贵都大饭店办公楼405单元  
Phone: +86-21-62489820  
Fax: +86-21-62489821

© 2012 The Author(s). Licensee IntechOpen. This is an open access article distributed under the terms of the [Creative Commons Attribution 3.0 License](#), which permits unrestricted use, distribution, and reproduction in any medium, provided the original work is properly cited.

IntechOpen

IntechOpen